Journal of Nuclear Medicine, published on July 19, 2013 as doi:10.2967/jnumed.112.118539

The Role of p53 in Combination Radioimmunotherapy with ^{64}Cu-DOTA-Cetuximab and Cisplatin in a Mouse Model of Colorectal Cancer

Yunjun Guo[1,2], Jesse J. Parry[3], Richard Laforest[1], Buck E. Rogers[3], and Carolyn J. Anderson[1,2,4,5]

[1]Mallinckrodt Institute of Radiology, Washington University, St. Louis, Missouri; [2]Department of Chemistry, Washington University, St. Louis, Missouri; [3]Department of Radiation Oncology, Washington University, St. Louis, Missouri; [4]Department of Biochemistry and Molecular Physics, Washington University, St. Louis, Missouri; and [5]Department of Radiology, University of Pittsburgh, Pittsburgh, Pennsylvania

Radioimmunotherapy has been successfully used in the treatment of lymphoma but thus far has not demonstrated significant efficacy in humans beyond disease stabilization in solid tumors. Radioimmunotherapy with ^{64}Cu was highly effective in a hamster model of colorectal cancer, but targeted radiotherapies with this radionuclide have since not shown as much success. It is widely known that mutations in key proteins play a role in the success or failure of cancer therapies. For example, the KRAS mutation is predictive of poor response to anti–epidermal growth factor receptor therapies in colorectal cancer, whereas p53 is frequently mutated in tumors, causing resistance to multiple therapeutic regimens. **Methods:** We previously showed that nuclear localization of ^{64}Cu-labeled DOTA-cetuximab was enhanced in p53 wild-type tumor cells. Here, we examine the role of p53 in the response to radioimmunotherapy with ^{64}Cu-DOTA-cetuximab in KRAS-mutated HCT116 tumor–bearing mice, with and without cisplatin, which upregulates wild-type p53. **Results:** Experiments with HCT116 cells that are p53 +/+ (p53 wild-type) and −/− (p53 null) grown in cell culture demonstrated that preincubation with cisplatin increased expression of p53 and subsequently enhanced localization of ^{64}Cu from ^{64}Cu-acetate and ^{64}Cu-DOTA-cetuximab to the tumor cell nuclei. Radioimmunotherapy studies in p53-positive HCT116 tumor–bearing mice, receiving either radioimmunotherapy alone or in combination with cisplatin, showed significantly longer survival in mice receiving unlabeled cetuximab or cisplatin alone or in combination (all, $P < 0.01$). In contrast, the p53-negative tumor-bearing mice treated with radioimmunotherapy alone or combined with cisplatin showed no survival advantage, compared with control groups (all, $P > 0.05$). **Conclusion:** Together, these data suggest that ^{64}Cu specifically delivered to epidermal growth factor receptor–positive tumors by cetuximab can suppress tumor growth despite the KRAS status and present opportunities for personalized clinical treatment strategies in colorectal cancer.

Key Words: radioimmunotherapy; KRAS mutation; colorectal cancer; ^{64}Cu

J Nucl Med 2013; 54:1–9
DOI: 10.2967/jnumed.112.118539

Received Dec. 14, 2012; revision accepted Apr. 12, 2013.
For correspondence or reprints contact: Carolyn J. Anderson, Department of Radiology, 100 Technology Dr., Ste. 452F, Pittsburgh, PA 15217.
E-mail: andersoncj@upmc.edu
Published online ■■■■■■■■■■■■.
COPYRIGHT © 2013 by the Society of Nuclear Medicine and Molecular Imaging, Inc.

Colorectal cancer remains the fourth most common malignancy worldwide and the third leading cause of cancer mortality in the United States (*1*). For decades, chemotherapy has been the backbone of treatment for colorectal cancer and is often combined with more directed strategies such as surgery and radiation therapy (*2*). The addition of cetuximab, a chimeric IgG1 monoclonal antibody against the epidermal growth factor receptor (EGFR) (*3*), to the current chemotherapy regimen has significantly improved the outcome in colorectal cancer treatment (*4,5*). However, it has been reported that the clinical response to cetuximab can be substantially impaired by mutations in the KRAS oncogene, because the mutation can lead to a constitutive activation that is independent from the EGFR-driven signaling cascade (*6*). The occurrence rate of mutations in the KRAS protooncogene is as high as 35%–40% (*7*), so there is an urgent need to develop salvage therapies for patients who have failed traditional chemotherapies and are diagnosed with KRAS-mutated tumors.

Radioimmunotherapy offers the opportunity to enhance the intrinsic cytotoxicity of antibodies by incorporating targeted radiation directly into the treatment regimen, which represents an alternative cancer treatment with high selectivity, versatile targeting strategies, and reduced side effects for the patient. Previous studies have demonstrated that ^{64}Cu (half-life, 12.7 h) is a promising radionuclide for radioimmunotherapy because of its suitable half-life and unique decay characteristics (*8–11*). ^{64}Cu decays by both β^+ (maximum energy [E_{max}], 656 keV; 17.4%) and β^- (E_{max}, 573 keV; 38.5%) particles, enabling simultaneous diagnostic PET imaging and radiotherapy. Moreover, during decay by electron capture, ^{64}Cu emits Auger and conversion electrons with high-linear-energy transfer and short tissue-penetration range. When localized in the nucleus, Auger electrons are potentially more cytotoxic than longer range β^-or β^+ particles (*12,13*). ^{64}Cu demonstrated efficacy for radioimmunotherapy comparable to ^{67}Cu (half-life, 60.2 h; 100% β^-) (*9*), but ^{64}Cu is more readily available in higher specific activity by medical cyclotron production, compared with ^{67}Cu, which can be made only in larger quantities on a very-high-energy cyclotron or accelerator (*14*).

One strategy to improve the outcome of radioimmunotherapy with ^{64}Cu is to enhance the localization of ^{64}Cu in tumor cell nuclei (*15*). There is evidence that the tumor-suppressor protein p53 plays an important role in the transport of ^{64}Cu to the cell nucleus, because enhanced ^{64}Cu nuclear localization is observed

jnm118539-pm ■ 7/19/13
Copyright 2013 by Society of Nuclear Medicine.

in tumors that express wild-type p53, compared with tumors that are null for p53 (*16*). On activation in response to DNA damage or other types of cellular stress, p53 accumulates in the cell nucleus where it transcriptionally triggers cell cycle inhibition, senescence, or apoptosis (*17*). As one of the most important proteins related to tumor growth, p53 has a crucial role in many cancer therapy regimens. Kabolizadeh et al. reported that p53 expression can alter the effects of copper on cisplatin-mediated cell death (*18*). In p53 wild-type human colorectal cancer cells (HCT116), the addition of copper decreased cisplatin-mediated cell death, yet the effect was lost in the absence of p53. Previous studies demonstrated that the major copper influx transporter 1 (CTR1) regulates tumor cell uptake of cisplatin, and the 2 copper efflux transporters ATP7A and ATP7B regulate the efflux of the drug (*19*).

^{64}Cu-DOTA-cetuximab was demonstrated to have high anti-EGFR immunoreactivity and effective tumor accumulation in several EGFR-positive tumors, including A431, CaSki, HCT116, and others (*16,20*). Using ^{64}Cu-DOTA-cetuximab, we investigated the effect of radioimmunotherapy with and without cisplatin in HCT116 human colorectal tumors that were wild-type or null for the tumor-suppressor protein p53.

MATERIALS AND METHODS

Chemicals and Reagents

^{64}Cu was produced on a biomedical cyclotron at the Washington University School of Medicine using published methods (*14*). DOTA was purchased from Macrocyclics, Inc. The p53 primary antibody was purchased from Santa Cruz Biotechnology. The protein content was determined using the BCA protein assay kit (Thermo Scientific), following the manufacturer's protocol. All other chemicals, including cisplatin, were purchased from Sigma-Aldrich Chemical Co. ^{64}Cu-DOTA-cetuximab was prepared according to literature methods (*21*), in specific activities ranging from 0.44 to 0.55 MBq/μg (12–15 μCi/μg).

In Vitro Studies

Human colorectal tumor cells that are p53 wild-type (HCT116 +/+) and p53 null (HCT116 −/−) were kindly provided by Dr. Bert Vogelstein at Johns Hopkins University. They were cultured with Dulbecco modified Eagle medium supplemented with 10% fetal bovine serum and 0.1% gentamicin in a 37°C humidified 95% air, 5% CO_2 incubator.

Whole-cell and nuclei lysates were blotted with mouse monoclonal antibody against p53 (Santa Cruz Biotechnology) and resolved with secondary antibody conjugated with horseradish peroxidase. Blots were treated with a chemiluminescent detection kit (Fisher Scientific) and exposed to films.

The nuclear fraction of HCT116 cells was isolated as previously described (*22*). Briefly, pelleted cells were resuspended in cytoskeletal (CSK) buffer (0.5% Triton X-100, 300 mM sucrose, 100 mM NaCl, 1 mM ethylene glycol tetraacetic acid [EGTA], 2 mM $MgCl_2$, and 10 mM *N,N′*-bis(2-ethanesulfonic acid) [PIPES], pH 6.8) and incubated on ice for 2 min. Cell lysates were centrifuged at 560*g* at 4°C for 5 min, and the supernatant was aspirated. The same procedure was repeated, except CSK buffer was used without Triton X-100. The whole-cell and nuclear pellets were counted for radioactivity in a γ-counter. Whole-cell internalization and nuclear uptake of ^{64}Cu were the amount of radioactivity in final cell or nuclei pellets, normalized to the protein content. *P* values were determined by a 2-way ANOVA test using Prism 5 (GraphPad).

Animal Studies

All animal experiments were conducted in compliance with the Guidelines for the Care and Use of Research Animals established by Washington University's Animal Studies Committee. Five- to 6-wk-old female athymic nude mice were purchased from the National Cancer Institute. For biodistribution studies and small-animal PET/CT imaging, HCT116 +/+ and −/− cells (4×10^6) in 100 μL of 0.9% saline were implanted subcutaneously into the dorsal flank of each animal, and the tumors were allowed to grow to a volume of 100–200 mm^3 (2–3 wk). For radioimmunotherapy studies, 2.5×10^6 HCT116 cells were injected into mice following the same protocol as above. One or 2 wk after implantation, mice were randomized into control and treatment groups when established tumors were palpable (20–50 mm^3).

PET imaging of tumor-bearing mice was done using the microPET Focus 120/220 or the Inveon PET small-animal scanners (Siemens Medical Solutions), and the CT data were collected using a microCAT II (Siemens Medical Solutions). The mice were intravenously injected with ^{64}Cu-DOTA-cetuximab, and static scans were acquired 24, 48, and 72 h after injection. Tumor standardized uptake values (SUVs) were generated by measuring regions of interest from PET/CT images and calculated with the formula SUV = [Bq/mL] × [animal weight (g)]/injected dose [Bq] decay-corrected to the scan time after injection.

In radioimmunotherapy studies, mice bearing HCT116 +/+ and −/− tumors implanted on the flank (1 tumor/mouse) were randomized into 7 groups and treated with 1 dose of agents according to the regimen illustrated in Table 1. Two rounds of treatment were administered 1 wk apart. The tumor volume was measured with calipers twice per week. When tumors reached a volume of 2,000 mm^3 or became ulcerated, mice were sacrificed by cervical dislocation while [**Table 1**]

TABLE 1
Treatment Groups for HCT116 +/+ and HCT116 −/− Tumor–Bearing Mice

Group	Injection
1	Intraperitoneal: 150 μL of saline
2	Intraperitoneal: cisplatin (5 mg/kg) in 150 μL of saline
3	Intravenous: 22.2 MBq (600 μCi) of ^{64}Cu-DOTA-cetuximab in 150 μL of saline
4	Intraperitoneal: cisplatin (5 mg/kg) in 150 μL of saline, followed by intravenous injection of 22.2 MBq (600 μCi) of ^{64}Cu-DOTA-cetuximab in 150 μL of saline after 24 h
5	Intravenous: 50 μg of cetuximab in 150 μL of saline
6	Intraperitoneal: cisplatin (5 mg/kg) in 150 μL of saline, followed by intravenous injection of 50 μg of cetuximab in 150 μL of saline after 24 h
7	Intravenous: 22.2 MBq (600 μCi) of ^{64}Cu-IgG in 150 μL of saline

Mice received 2 treatments 1 wk apart for each group.

jnm118539-pm ■ 7/19/13

under anesthesia. *P* values for survival curves were determined by a log-rank (Mantel–Cox) test using Prism 5.

Human Dosimetry Calculations

The estimated human absorbed doses of ^{64}Cu-DOTA-cetuximab to normal organs were obtained using biodistribution data in HCT116 +/+ tumor–bearing mice, according to methods described previously (*20*). ^{64}Cu-DOTA-cetuximab (740–1,110 kBq) in 150 μL of saline was injected via the tail vein, and blood, organs, and tumors were removed from mice sacrificed at 1, 4, 24, 48, and 72 h after injection ($n = 5$ for each time point). The mice were housed for 72 h in metabolism cages to determine the percentage injected dose excreted in urine and feces at every time point. The radiation-absorbed doses of each organ were calculated on the basis of previously published methods (*11*). Briefly, time–activity curves were generated by nonlinear regression fit of decay-corrected percentage injected dose per organ to time after injection. Residence times were calculated on the basis of the time–activity curve and then incorporated into the OLINDA program (Vanderbilt University, http://www.doseinfo-radar.com/OLINDA.html) to obtain the radiation dose (rad/mCi or mGy/MBq) for each organ and whole-body effective dose. Bone activity was assumed to be distributed equally between the trabecular bone and cortical bone. Feces and urine were collected and used to calculate the excreted residence time. All the unobserved activity was associated with the remainder of the body. No urine or fecal excretion was collected in the course of the experiment because excretion is expected to be low for a monoclonal antibody.

The integrated cumulative time–activity in the HCT116 +/+ tumor model was measured from the animal biodistribution data. The dose to the tumor was calculated from the product of the tumor residence time assuming a 1-g tumor and the ^{64}Cu dose rate obtained from the sphere model in OLINDA/EXM.

RESULTS

Cisplatin-Activated p53 Expression in HCT116 p53 Wild-Type Cells

To investigate the relationship between cisplatin and p53 expression level in HCT116 cells, we measured the p53 activation by Western blot analysis. Cisplatin treatment induced robust p53 expression in HCT116 cells, in both whole-cell pellets and pure nuclear fractions (Supplemental Fig. 1; supplemental materials are available at http://jnm.snmjournals.org). The optimal concentration of cisplatin for activating p53 expression was determined to be 40 μM. A time course where 40 μM cisplatin was incubated with cells demonstrated that 20 h was the optimal incubation time for subsequent studies.

Cisplatin-Activated Nuclear Localization of ^{64}Cu-Acetate and ^{64}Cu-DOTA-Cetuximab

Similar amounts of ^{64}Cu accumulated in the nuclei of both lines without cisplatin (2.1% ± 0.5% in HCT116 +/+ vs. 2.3% ± 0.5% in HCT116 −/−) (Fig. 1A). The addition of cisplatin enhanced the nuclear uptake of ^{64}Cu in HCT116 +/+ cells by nearly 4.5-fold ($P < 0.0001$), because 9.2% ± 1.5% of internalized ^{64}Cu was transported into the nucleus over 20 h. However, cisplatin did not affect ^{64}Cu nuclear localization in p53-negative cells (2.3% ± 0.5% without cisplatin vs. 2.5% ± 0.3% with cisplatin). [**Fig. 1**]

Similar results were observed when ^{64}Cu was administered in the form of ^{64}Cu-DOTA-cetuximab (Fig. 1B). The addition of cisplatin increased nuclear uptake of ^{64}Cu in HCT116 +/+ cells from 12.1% ± 0.9% to 40.7% ± 6.8% ($P < 0.0001$). In contrast, the amount of ^{64}Cu localized in the nuclei of HCT116 −/− cells was essentially unchanged after the addition of cisplatin (13.7% ± 1.6% without cisplatin vs. 13.3% ± 1.9% with cisplatin). The p53

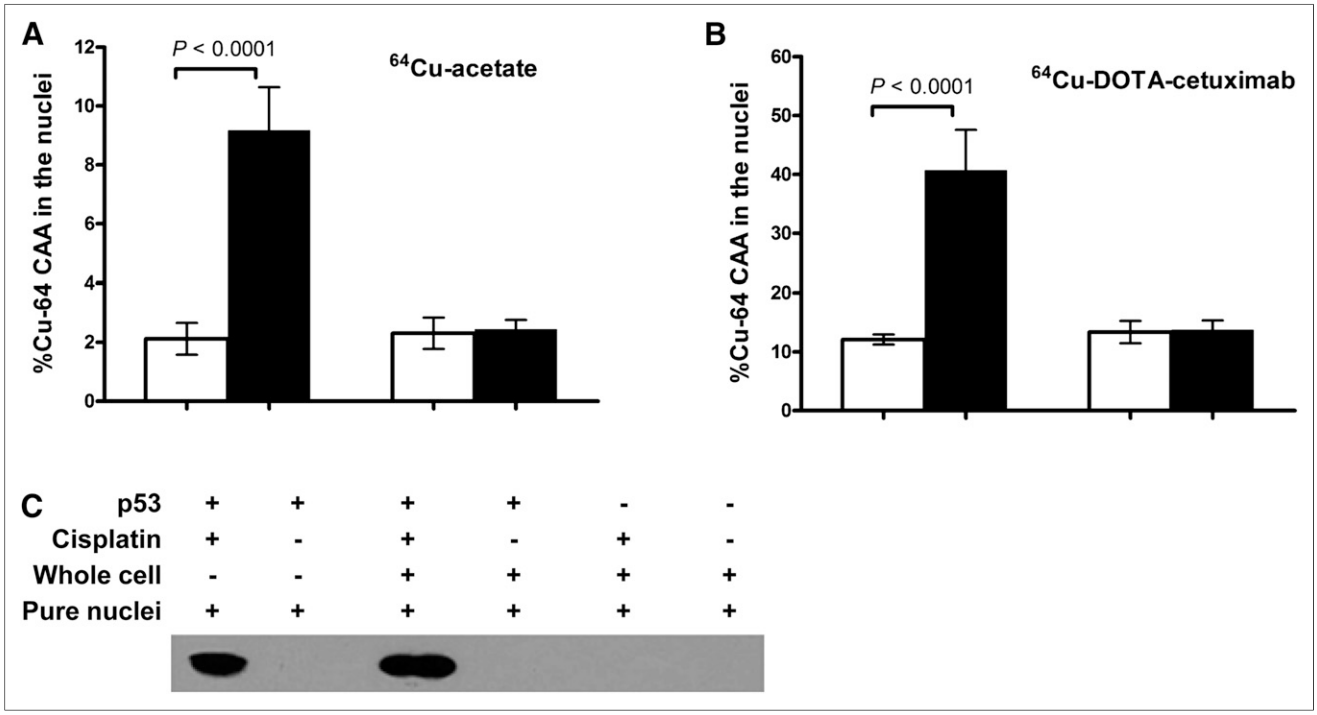

FIGURE 1. Effect of cisplatin on nuclear uptake of ^{64}Cu in p53 wild-type and null HCT116 cell lines. HCT116 cells were incubated with or without 40 μM cisplatin before incubation with ^{64}Cu-acetate (A) or ^{64}Cu-DOTA-cetuximab (B) for another 20 h. (C) Expression level of p53 in HCT116 cells cultured with ^{64}Cu-DOTA-cetuximab, either with or without prior incubation with cisplatin, was detected by Western blot. Amount of p53 detected in both whole cells and pure nuclei are shown.

expression levels in the 2 cell lines were determined by Western blot analysis. The addition of cisplatin significantly upregulated p53 in cytosol and nuclei of HCT116 +/+ cells (Fig. 1C). There was no visible p53 in HCT116 −/− whole cells or nuclei.

In Vivo Mouse Biodistribution and Dosimetry

The biodistribution study of ^{64}Cu-DOTA-cetuximab was conducted in HCT116 +/+ tumor–bearing nude mice (Fig. 2). The tumor uptake of ^{64}Cu-DOTA-cetuximab in HCT116 +/+ tumor–bearing nude mice steadily increased from 1 to 72 h after injection. ^{64}Cu-DOTA-cetuximab demonstrated a slow blood clearance. The specificity of ^{64}Cu-DOTA-cetuximab for EGFR on HCT116 +/+ tumor cells was confirmed by injection of an excess amount of unlabeled cetuximab 24 h before the tracer injection.

Human absorbed dose estimates to normal organs were calculated from the above mouse biodistribution data (Supplemental Table 1). Organ doses are presented in Table 2. The absorbed dose to the liver for ^{64}Cu-DOTA-cetuximab was 0.12 mGy/MBq (0.43 rad/mCi). The intestinal tract showed prominent uptake, because the absorbed dose to the lower large intestine wall is highest among all the organs (lower large intestine wall, 0.14 mGy/MBq [0.53 rad/mCi]). The whole-body effective dose was 0.03 mGy/MBq (0.12 rad/mCi). The absorbed doses to other organs, such as kidneys, pancreas, and spleen, were all determined to be close to the whole-body dose at approximately 0.027 mGy/MBq (0.1 rad/mCi), whereas the dose to the red marrow was 0.046 mGy/MBq (0.171 rad/mCi). The absorbed dose of the HCT116 +/+ tumor was 105 mGy/MBq (390 rad/mCi). This value is assumed to be the same with HCT116 −/− tumors because the total number of EGFR binding sites on HCT116 +/+ cells and HCT116 −/− cells was determined to be similar (*16*), and a biodistribution study conducted with mice bilaterally implanted with both HCT116 +/+ and HCT116 −/− tumors showed the tumor uptake to not be statistically different (P = 0.07 at 24 h; P = 0.8 at 72 h) (Fig. 2C).

Small-Animal PET/CT Imaging

Small-animal PET/CT images of ^{64}Cu-DOTA-cetuximab at 24, 48, and 72 h clearly visualized HCT116 +/+ tumors (Fig. 3A), both with and without cetuximab (Fig. 3B). A significant reduction of tumor uptake was observed in mice receiving a blocking dose of unlabeled cetuximab, consistent with results from the biodistribution study. A good agreement between the SUV analysis and the biodistribution study was observed (Fig. 3C); there was a steady increase of tumor uptake from 24 to 72 h, and the preinjection of unlabeled cetuximab reduced tumor uptake by at least 70%.

The distribution pattern of ^{64}Cu-DOTA-cetuximab with or without pretreatment of cisplatin was similar. The radiopharmaceutical selectively accumulated in the tumor and gradually became the only clearly visible tissue after the tracer cleared from the liver. Cisplatin did not lead to an enhancement of the tumor accumulation of ^{64}Cu-DOTA-cetuximab. In contrast, the SUV of tumors treated with cisplatin was slightly, but not significantly, lower than the tumor without treatment at 48 and 72 h after the administration of ^{64}Cu-DOTA-cetuximab.

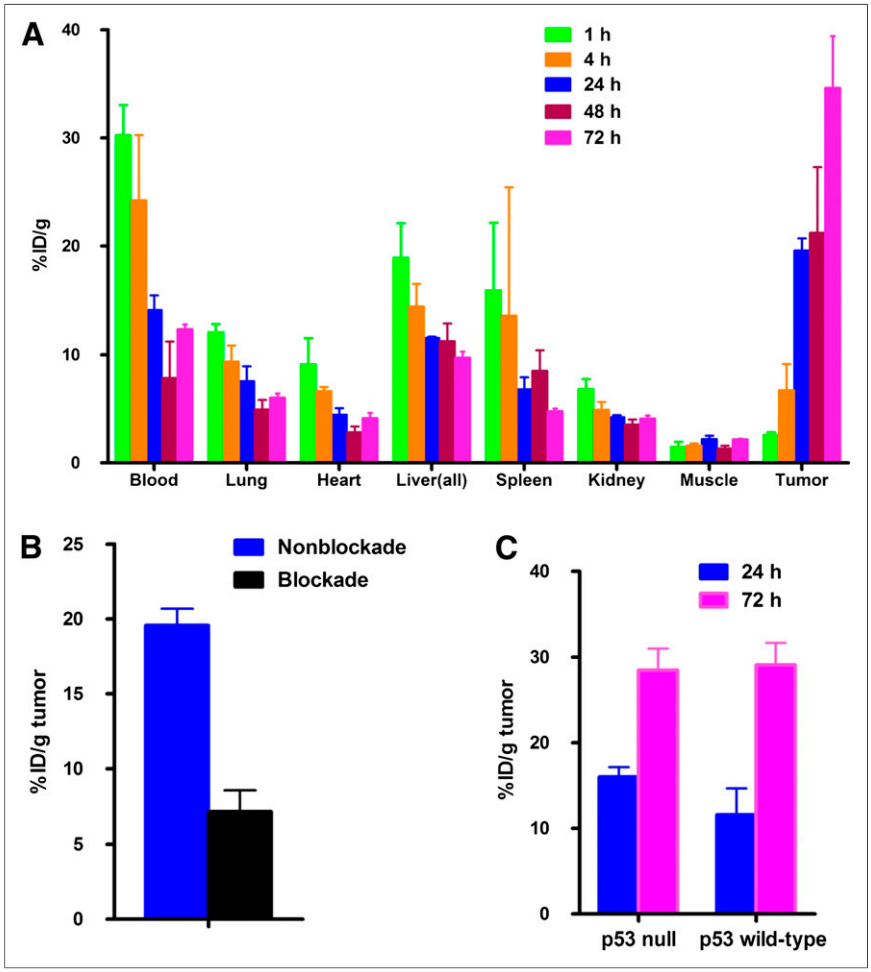

FIGURE 2. (A) Biodistribution of ^{64}Cu-DOTA-cetuximab in HCT116 +/+ tumor–bearing nude mice. Data are presented as percentage injected dose per gram (%ID/g) ± SD (n = 5 for each time point). (B) One milligram of unlabeled cetuximab was injected to each mouse 24 h before administration of radiotracer to block specific uptake of ^{64}Cu-DOTA-cetuximab ($P < 0.001$). (C) Mice bilaterally implanted with both HCT116 +/+ and HCT116 −/− tumors showed tumor uptake to be similar (P = 0.07 at 24 h after injection, P = 0.8 at 72 h after injection).

Radioimmunotherapy of ^{64}Cu-DOTA-Cetuximab in HCT116 +/+ and HCT116 −/− Tumor–Bearing Mice

HCT116 +/+ tumor–bearing mice treated with ^{64}Cu-DOTA-cetuximab demonstrated an inhibition of tumor growth for up to 17 d after the second injection of ^{64}Cu-DOTA-cetuximab (Fig. 4). By day 32, all mice treated with saline had to be sacrificed because the tumors had grown more than 2 g. In contrast, 100% of mice treated with ^{64}Cu-DOTA-cetuximab were still alive. The radioimmunotherapy regimen improved the median survival of HCT116 +/+ tumor–bearing mice from 28 d in the saline-treated group to 52 d in mice treated with ^{64}Cu-DOTA-cetuximab

jnm118539-pm ■ 7/19/13

TABLE 2
Human Absorbed Dose Estimates Determined by Mouse Biodistribution Data

Organ	Dose	
	mGy/MBq	rad/mCi
Lower large intestine wall	0.14	0.525
Small intestine	0.030	0.111
Stomach wall	0.044	0.163
Upper large intestine wall	0.083	0.308
Kidneys	0.043	0.160
Liver	0.12	0.434
Lungs	0.028	0.103
Pancreas	0.030	0.111
Red marrow	0.046	0.171
Spleen	0.066	0.244
Osteogenic cells	0.11	0.414
Heart wall	0.085	0.315
Urinary bladder wall	0.026	0.096
Total body	0.032	0.118

Effective dose was 0.050 mSv/MBq (0.183 [rem/mCi]).

[**Fig. 5**] ($P < 0.0001$) (Fig. 5). To our surprise, the addition of cisplatin to the radioimmunotherapy regimen showed no significant difference in overall survival ($P = 0.61$). The treatment of unlabeled cetuximab alone showed a moderate inhibition of tumor growth, compared with tumors treated with saline ($P < 0.05$), with a median survival of 32 d, whereas ^{64}Cu-DOTA-cetuximab significantly inhibited tumor growth, compared with unlabeled cetuximab ($P < 0.0001$). For example, on day 28, the average tumor volume in the ^{64}Cu-DOTA-cetuximab group was 3-fold smaller than that in mice treated with unlabeled cetuximab. Moreover, the median survival of mice treated with ^{64}Cu-DOTA-cetuximab was improved by 20 d, compared with mice treated with unlabeled cetuximab. The addition of cisplatin to unlabeled cetuximab did not significantly increase overall survival ($P = 0.25$) but slightly elongated the median survival by 2 d. The median survival of ^{64}Cu-IgG–treated mice was 6 d longer than that of saline-treated mice ($P < 0.01$) and 18 d shorter than that of ^{64}Cu-DOTA-cetuximab–treated mice ($P < 0.001$), respectively, demonstrating that nonspecific ^{64}Cu-labeled proteins are not as effective. Mice were monitored for weight loss and lethargy, and no significant toxicity was observed for any of the treatments.

In contrast to p53 +/+ tumor–bearing mice, the treatment of ^{64}Cu-labeled cetuximab in p53 −/− mice did not result in significant tumor inhibition (Fig. 4). The average tumor volume of saline-treated mice was comparable to that of ^{64}Cu-DOTA-cetuximab–treated mice at all days after tumor implantation. Although radioimmunotherapy in the p53 −/− mice extended the median survival of tumor-bearing mice from 36 to 39 d, the log-rank test showed no significant difference between the 2 groups ($P = 0.09$) (Fig. 5). Unlabeled cetuximab showed no therapeutic effect for p53 −/− tumors. The combination of chemotherapy and radioimmunotherapy also did not provide any beneficial effect, and there was no significant improvement of median survivals observed between mice treated with ^{64}Cu-DOTA-cetuximab and those treated with ^{64}Cu-DOTA-cetuximab plus cisplatin ($P = 0.36$).

Soon after the first injection, ^{64}Cu-DOTA-cetuximab, alone or combined with cisplatin, showed substantial tumor inhibition for HCT116 +/+ mice on each day of measurement, and the effect continued until 17 d after the second injection of radioimmunotherapy. In contrast, ^{64}Cu-DOTA-cetuximab did not give notable benefit for HCT116 −/− mice during the entire radioimmunotherapy treatment. On day 28 after implantation of HCT116 +/+ tumors, only 3 of 8 mice in the saline-treated control group were still alive, with the average tumor volume of 2,200 ± 300 mm^3. The average tumor volume of the group treated with ^{64}Cu-DOTA-cetuximab was 450 ± 70 mm^3 and that of the group treated with ^{64}Cu-DOTA-cetuximab plus cisplatin was 400 ± 70 mm^3 (all P values < 0.01, compared with saline controls). The average volume of saline-treated HCT116 −/− tumors 29 d after implantation was 1,300 ± 110 mm^3, demonstrating a slower natural growth rate than for p53 wild-type tumors ($P < 0.05$). The average volume of HCT116−/− tumors treated by ^{64}Cu-DOTA-cetuximab was 1,100 ± 70 mm^3 and that treated by ^{64}Cu-DOTA-cetuximab plus cisplatin was 1,000 ± 350 mm^3. Radioimmunotherapy led to a slight but not significant reduction in tumor sizes, compared with other control groups (all P values > 0.05).

DISCUSSION

Radioimmunotherapy and targeted radiotherapy with ^{64}Cu-labeled tumor-targeting antibodies and peptides have shown efficacy in inhibiting tumor growth and preventing peritoneal spread of cancer cells in mouse models of cancer (*10,11,23,24*). Because of the unique decay scheme of ^{64}Cu, its cytotoxicity can be enhanced by intracellular decay, especially near the cell nucleus (*15*). We have shown previously that the presence of the tumor-suppressor protein p53 enhanced nuclear localization of ^{64}Cu in HCT116 tumor cells. In the present study, we aimed at developing a combined chemotherapy with cisplatin and targeted radioimmunotherapy with a ^{64}Cu-DOTA-cetuximab treatment regimen in a mouse model of KRAS-mutated colorectal cancer.

The cytotoxicity of cisplatin is primarily mediated by its interaction with DNA to form DNA adducts, which activate several signal transduction pathways in a heavily p53-dependent manner (*25*). The presence of wild-type p53 was positively correlated to sensitivity to cisplatin in a National Cancer Institute panel of 60 human tumor cell lines (*26*). Western blot analysis demonstrated that cisplatin robustly induced p53 expression in HCT116 tumor cells. It is well established that p53 is unstable and quickly degrades in the absence of stress factors. Accumulation of p53 is induced under stress conditions, such as ultraviolet or γ-irradiation, low oxygen, and toxins (*27*). DNA damage caused by the formation of cisplatin–DNA adducts leads to stabilization and subsequent accumulation of p53 protein in p53 wild-type HCT116 tumor cells.

We previously presented data showing that p53 is directly or indirectly involved in the process of copper transport to tumor cell nuclei (*16*). Because cisplatin was demonstrated to increase expression of p53 in HCT116 +/+ cells, we hypothesized that cisplatin could also upregulate the amount of ^{64}Cu entering tumor cell nuclei. Despite the different cellular uptake mechanism of ^{64}Cu-acetate (via CTR1 transporter) and ^{64}Cu-DOTA-cetuximab (via EGFR-mediated endocytosis), we observed significant enhancement of nuclear uptake of ^{64}Cu by the addition of cisplatin only in p53 wild-type HCT116 cells for the 2 radiopharmaceuticals. In p53-null HCT116 cells, the amount of ^{64}Cu activity located in the tumor cell nuclei was similar with or without cisplatin. Moreover, when no cisplatin was added to the cells, the

jnm118539-pm ■ 7/19/13

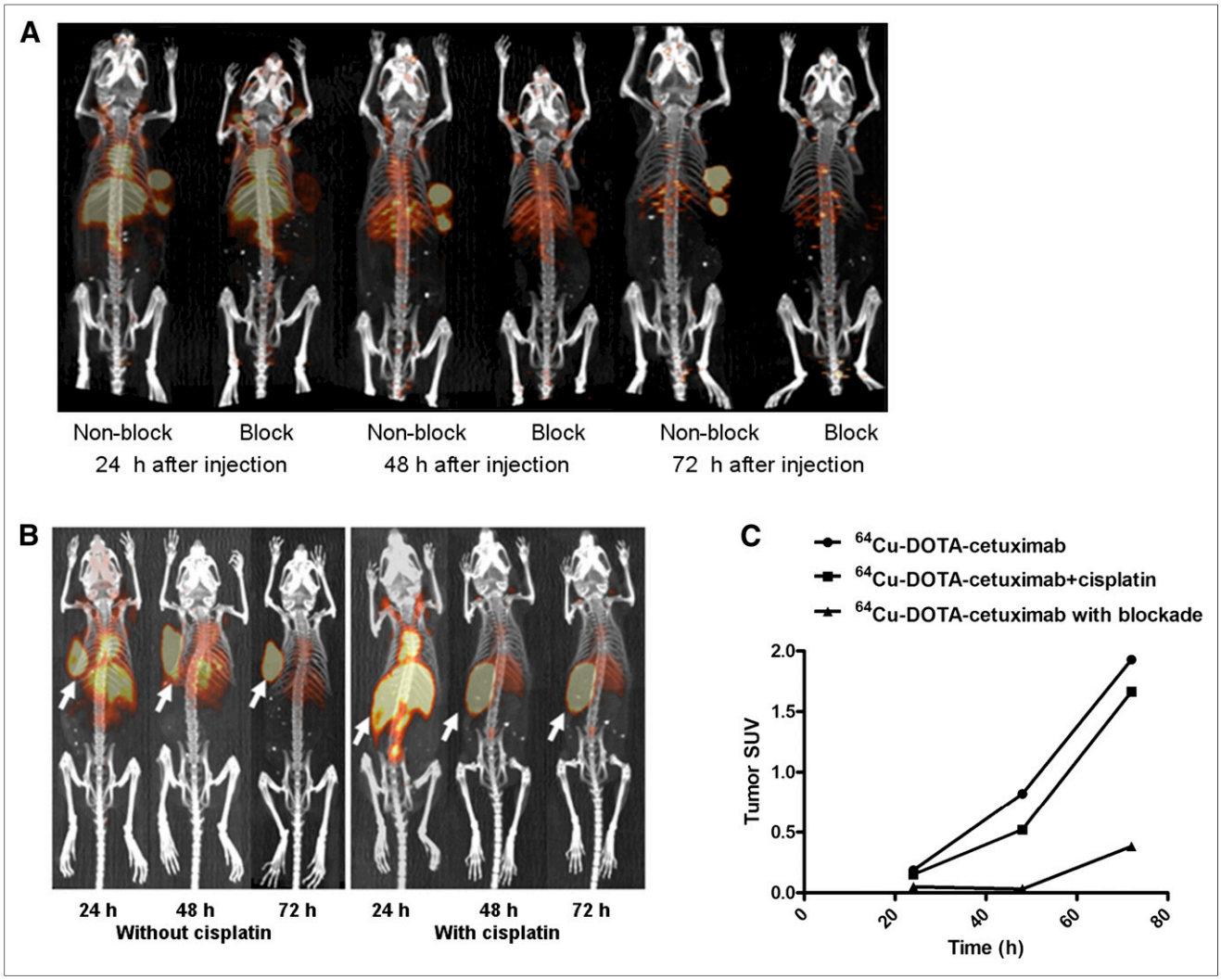

FIGURE 3. (A) Small-animal PET/CT projection images of HCT116 +/+ tumor–bearing nude mice at 24, 48, and 72 h after injection of ^{64}Cu-DOTA-cetuximab, with or without 24 h preinjection of excess amount of unlabeled cetuximab. (B) Small-animal PET/CT projection images of HCT116 +/+ tumor–bearing nude mice at 24, 48, and 72 h after injection of ^{64}Cu-DOTA-cetuximab, with or without 24 h preinjection of cisplatin (5 mg/kg). (C) SUVs were determined from quantifying activity in regions of interest from PET images of HCT116 +/+ tumor–bearing nude mice.

amounts of ^{64}Cu associated with the cell nucleus were comparable for the p53 +/+ and −/− cell lines. This observation is consistent with the fact that p53 is maintained at low levels in the absence of cellular stress. These data confirm our previous finding that p53 is involved in the trafficking pathway of copper into tumor cell nuclei. One possible mechanism is that p53 itself complexes copper and carries it into the tumor cell nuclei. Because p53 is a crucial transcriptional factor that affects many cellular processes, another possibility is that one of the downstream proteins of p53 is responsible for transporting copper into tumor cell nuclei. Research into finding the protein responsible for transporting copper into the tumor cell nucleus is under way.

The treatment efficacy of combining cetuximab with standard chemotherapy for colorectal cancer has been evaluated in several clinical trials, and the clinical outcome was shown to be significantly improved in certain subgroups of patients (*28*). Additional analysis evaluating the relationship between the response rate to cetuximab-added therapy and KRAS status revealed that the benefit from cetuximab is restricted to patients with a wild-type KRAS gene (*29*). For example, in the CRYSTAL study (Cetuximab Combined with Irinotecan in First-Line Therapy for Metastatic Colorectal Cancer) (*30*), the benefit of adding cetuximab to the folinic acid, fluorouracil, irinotecan (FOLFIRI) chemotherapy was observed only in the group of patients with wild-type KRAS, whereas in the KRAS-mutated group, the response rate and median progression-free survival were worse in the cetuximab arm (*31*). An advantage of radiolabeled cetuximab over conventional cetuximab treatment is that it may be effective in patients with the mutated KRAS gene. Because the cytotoxicity of cetuximab comes from the blockade of EGFR and subsequent inhibition of downstream signaling pathways that heavily involve the KRAS gene, mutations in KRAS may bypass the EGFR signaling pathway and inhibit the clinical response to EGFR inhibitors (*32*). In the case of radiolabeled cetuximab, the cytotoxicity comes from the radiation dose specifically delivered to the tumor site rather than the cetuximab itself, as the median survival was improved from 28 d treated by

jnm118539-pm ■ 7/19/13

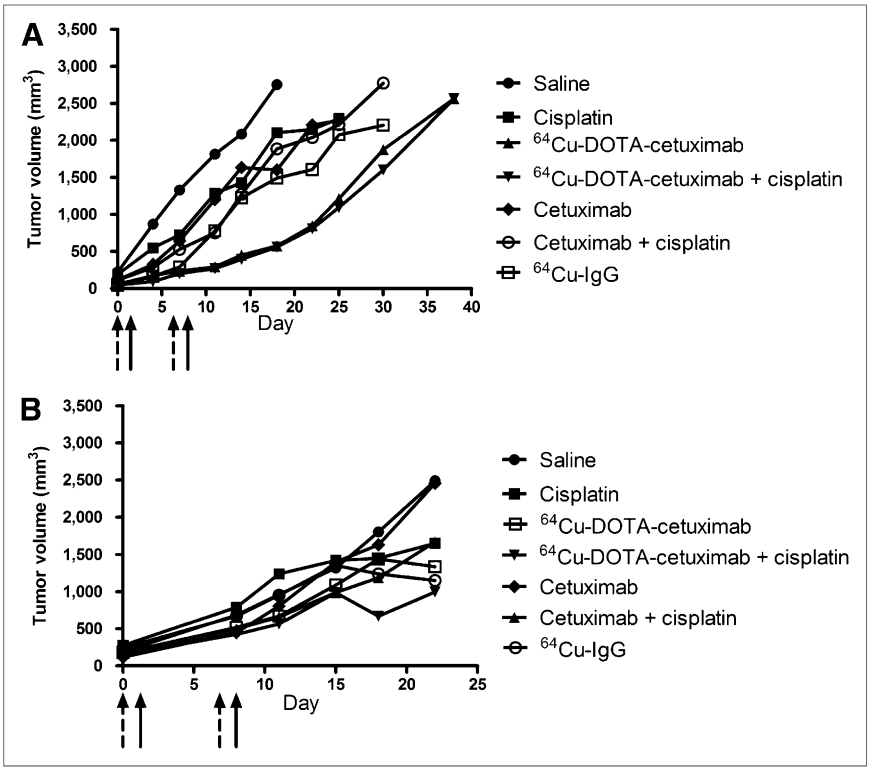

FIGURE 4. Radioimmunotherapy experiments in HCT116 +/+ (A) and HCT116 −/− (B) tumor–bearing nude mice. Comparison of average tumor growth in treated and control groups was shown. Tumor growth in individual mice of treated and control group was included in supplemental figures. Dash arrows = days when cisplatin was given; solid arrows = days when radioimmunotherapy was given.

saline to 32 d treated by cetuximab. Moreover, the treatment of unlabeled cetuximab did not lead to any benefit for p53-null HCT116 tumors. This is not surprising because HCT116 cell line has a mutation in codon 13 of the KRAS protooncogene (*33*). In contrast, the administration of the same amount of ^{64}Cu-DOTA-cetuximab improved the median survival of HCT116 +/+ tumor–bearing mice by 24 d over the saline-treated group. These data suggest that ^{64}Cu specifically delivered to EGFR-positive tumors by cetuximab can suppress tumor growth regardless of the KRAS status. Therefore, radiolabeled cetuximab may provide a future option for KRAS-mutated patients with p53-positive tumors who have failed both traditional and cetuximab-combination chemotherapy.

Recently, Huang et al. reported that p53 plays a central role in regulating acquired resistance to EGFR inhibitors and radiation (*34*). By knocking down p53 in sensitive parental cells, they showed a reduction in efficacy to both cetuximab and radiation. Moreover, restoration of functional p53 in EGFR inhibitor–resistant cells was sufficient to resensitize them to cetuximab and radiation in vivo and in vitro. Previous studies showed that cetuximab inhibits the growth of p53 wild-type but not p53-mutated cancer cells and fostered the hypothesis that resistance to cetuximab may be related to p53 mutation (*35*). Consistent with their findings, we found that p53 status affected the response of HCT116 tumor cells to both unlabeled and ^{64}Cu-labeled cetuximab. Unlabeled cetuximab did not lead to significant benefit for either p53 +/+ or −/− tumor–bearing mice, most likely because of the KRAS mutation. Nonetheless, p53-null tumors were still shown to be slightly more resistant to cetuximab than p53 wild-type tumors. The increased survival in p53 +/+ tumors in mice treated with ^{64}Cu-labeled cetuximab, compared with control agents, was substantial, consistent with the previous finding that the expression of wild-type p53 is required for the efficacy of radiation therapy (*36,37*). Results from our study suggest opportunities to design personalized radioimmunotherapy for patients with EGFR-positive colorectal tumors according to the p53 expression level, even if the tumor has the KRAS mutation.

Human radiation dose estimates from mouse biodistribution data indicate the largest radiation dose is to the liver and the large intestine at 0.12 mGy/MBq (0.43 rad/mCi) and 0.14 mGy/MBq (0.53 rad/mCi). No excretion in urine and feces was observed. The effective dose was calculated to be 0.050 mSv/MBq (0.18 rem/mCi). Under Title 21 CFR 361.1 specifications, an injected dose of approximately 370 MBq (10 mCi) of ^{64}Cu-DOTA-cetuximab would yield a limiting dose of 53 and 43 mSv (5.3 and 4.3 rads) to the lower large intestine and liver, respectively, and an effective dose of 18 mSv (1.8 rem) for an adult male subject. In comparison, the adult effective dose for ^{18}F-FDG is 0.019 mSv/MBq (*38*), which translates into 10.5 mSv for a 550-MBq (15 mCi) study. On the basis of these preliminary dosimetry data in mice, there should be no barriers for PET imaging in humans with ^{64}Cu-DOTA-cetuximab.

Radioimmunotherapy with ^{64}Cu-DOTA-cetuximab may also be feasible in humans. Mice received up to 2 injections of 22.2 MBq (0.6 mCi), with no observable side effects, which would scale up to 62 GBq (1,680 mCi) per injection in humans. The red marrow would be the dose-limiting organ for radioimmunotherapy studies, because it is well known that the maximum tolerated dose in this organ is reached at a lower absorbed dose than other organs (*39*). On the basis of the dosimetry data presented here, the estimated dose to the red marrow would be 2,860 mSv (286 rad), which is in the range of 3,000 mSv (300 rad) to the marrow that has been shown to induce a 1% chance of leukemia within 10 y after exposure. Although a red marrow dose of 2,860 mSv (286 rad) is relatively high, fractionation of the ^{64}Cu-DOTA-cetuximab might mitigate the marrow toxicity.

CONCLUSION

We presented in vitro data that confirmed our previous hypothesis that p53 is involved in the trafficking pathway of copper into tumor cell nuclei. The results from in vivo therapy studies in HCT116 +/+ tumor–bearing mice demonstrate great potential of ^{64}Cu-DOTA-cetuximab for treating p53 wild-type EGFR-positive colorectal tumors regardless of the KRAS status. However, the combination of cisplatin with radioimmunotherapy did not show increased efficacy, compared with radioimmunotherapy

jnm118539-pm ■ 7/19/13

RGB

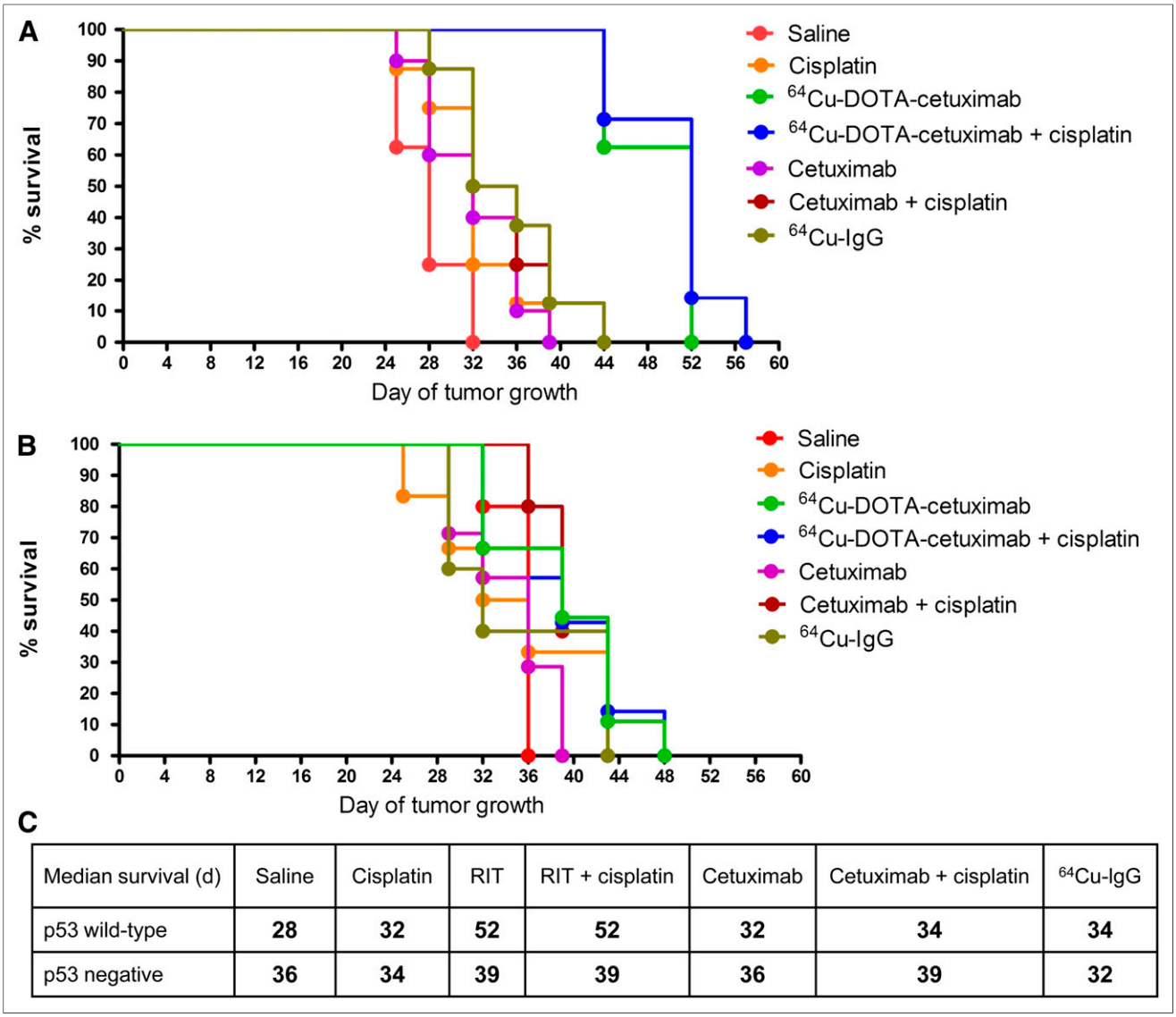

C

Median survival (d)	Saline	Cisplatin	RIT	RIT + cisplatin	Cetuximab	Cetuximab + cisplatin	^{64}Cu-IgG
p53 wild-type	**28**	**32**	**52**	**52**	**32**	**34**	**34**
p53 negative	**36**	**34**	**39**	**39**	**36**	**39**	**32**

FIGURE 5. Effect of p53 status in p53 wild-type (A) and p53-null (B) tumors on survival of HCT116 tumor–bearing nude mice in treated and control groups. Estimated survival distribution function was generated using Kaplan–Meier time-to-death analysis. Median survivals of all treated and control groups with HCT116 +/+ and HCT116 −/− tumors are summarized in C. ***$P < 0.001$ vs. radioimmunotherapy group. **$P < 0.01$ vs. radioimmunotherapy group. RIT = radioimmunotherapy.

alone. Furthermore, we observed a much greater overall survival benefit of radioimmunotherapy in the p53 wild-type than in the p53-null HCT116 tumor–bearing mice. The results reported here present opportunities for personalized clinical treatment strategies that incorporate EGFR-targeting radioimmunotherapy.

DISCLOSURE

The costs of publication of this article were defrayed in part by the payment of page charges. Therefore, and solely to indicate this fact, this article is hereby marked "advertisement" in accordance with 18 USC section 1734. This study was supported in part by NIH NCI 5R01CA064475, and DESC0002032. The Siteman Cancer Center is supported in part by an NCI Cancer Center Support Grant no. P30 CA91842. No other potential conflict of interest relevant to this article was reported.

ACKNOWLEDGMENTS

We thank Margaret Morris and Nicole Fettig for their technical support. We also thank the Alvin J. Siteman Cancer Center at Washington University School of Medicine and Barnes-Jewish Hospital in St. Louis, MO, for the use of the Small Animal Cancer Imaging Core.

REFERENCES

1. Serrano C, Markman B, Tabernero J. Integration of anti-epidermal growth factor receptor therapies with cytotoxic chemotherapy. *Cancer J.* 2010;16:226–234.
2. Chau I, Cunningham D. Treatment in advanced colorectal cancer: what, when and how? *Br J Cancer.* 2009;100:1704–1719.
3. Jonker DJ, O'Callaghan CJ, Karapetis CS, et al. Cetuximab for the treatment of colorectal cancer. *N Engl J Med.* 2007;357:2040–2048.
4. Hurwitz H, Fehrenbacher L, Novotny W, et al. Bevacizumab plus irinotecan, fluorouracil, and leucovorin for metastatic colorectal cancer. *N Engl J Med.* 2004;350:2335–2342.

jnm118539-pm ■ 7/19/13

5. Cunningham D, Humblet Y, Siena S, et al. Cetuximab monotherapy and cetuximab plus irinotecan in irinotecan-refractory metastatic colorectal cancer. *N Engl J Med.* 2004;351:337–345.
6. Schubbert S, Shannon K, Bollag G. Hyperactive ras in developmental disorders and cancer. *Nat Rev Cancer.* 2007;7:295–308.
7. Bos JL, Fearon ER, Hamilton SR, et al. Prevalence of ras gene mutations in human colorectal cancers. *Nature.* 1987;327:293–297.
8. Anderson CJ, Jones LA, Bass LA, et al. Radiotherapy, toxicity and dosimetry of copper-64-TETA-octreotide in tumor-bearing rats. *J Nucl Med.* 1998;39: 1944–1951.
9. Connett JM, Anderson CJ, Guo LW, et al. Radioimmunotherapy with a ^{64}Cu-labeled monoclonal antibody: a comparison with ^{67}Cu. *Proc Natl Acad Sci USA.* 1996;93:6814–6818.
10. Connett JM, Buettner TL, Anderson CJ. Maximum tolerated dose and large tumor radioimmunotherapy studies of ^{64}Cu-labeled monoclonal antibody 1A3 in a colon cancer model. *Clin Cancer Res.* 1999;5:3207s–3212s.
11. Lewis JS, Lewis MR, Cutler PD, et al. Radiotherapy and dosimetry of ^{64}Cu-TETA-Tyr3-octreotate in a somatostatin receptor-positive, tumor-bearing rat model. *Clin Cancer Res.* 1999;5:3608–3616.
12. Adelstein SJ, Merrill C. Sosman Lecture. The Auger process: a therapeutic promise? *AJR.* 1993;160:707–713.
13. O'Donoghue JA, Wheldon TE. Targeted radiotherapy using Auger electron emitters. *Phys Med Biol.* 1996;41:1973–1992.
14. McCarthy DW, Shefer RE, Klinkowstein RE, et al. Efficient production of high specific activity ^{64}Cu using a biomedical cyclotron. *Nucl Med Biol.* 1997;24:35–43.
15. Boswell CA, Brechbiel MW. Auger electrons: lethal, low energy, and coming soon to a tumor cell nucleus near you. *J Nucl Med.* 2005;46:1946–1947.
16. Eiblmaier M, Meyer LA, Anderson CJ. The role of p53 in the trafficking of copper-64 to tumor cell nuclei. *Cancer Biol Ther.* 2008;7:63–69.
17. Vousden KH, Lu X. Live or let die: the cell's response to p53. *Nat Rev Cancer.* 2002;2:594–604.
18. Kabolizadeh P, Ryan J, Farrell N. Differences in the cellular response and signaling pathways of cisplatin and BBR3464 ([[trans-PtCl(NH3)(2)]2mu-(trans-Pt(NH3)(2)(H2N(CH2)(6)-NH2)2)]4+) influenced by copper homeostasis. *Biochem Pharmacol.* 2007;73:1270–1279.
19. Safaei R, Howell SB. Copper transporters regulate the cellular pharmacology and sensitivity to Pt drugs. *Crit Rev Oncol Hematol.* 2005;53:13–23.
20. Eiblmaier M, Meyer LA, Watson MA, Fracasso PM, Pike LJ, Anderson CJ. Correlating EGFR expression with receptor-binding properties and internalization of ^{64}Cu-DOTA-cetuximab in 5 cervical cancer cell lines. *J Nucl Med.* 2008;49:1472–1479.
21. Ping Li W, Meyer LA, Capretto DA, Sherman CD, Anderson CJ. Receptor-binding, biodistribution, and metabolism studies of ^{64}Cu-DOTA-cetuximab, a PET-imaging agent for epidermal growth-factor receptor-positive tumors. *Cancer Biother Radiopharm.* 2008;23:158–171.
22. Wang M, Caruano AL, Lewis MR, Meyer LA, VanderWaal RP, Anderson CJ. Subcellular localization of radiolabeled somatostatin analogues: implications for targeted radiotherapy of cancer. *Cancer Res.* 2003;63:6864–6869.
23. Lewis JS, Connett JM, Garbow JR, et al. Copper-64-pyruvaldehyde-bis(N(4)-methylthiosemicarbazone) for the prevention of tumor growth at wound sites following laparoscopic surgery: monitoring therapy response with microPET and magnetic resonance imaging. *Cancer Res.* 2002;62:445–449.
24. Lewis JS, Srinivasan A, Schmidt MA, Anderson CJ. In vitro and in vivo evaluation of ^{64}Cu-TETA-Tyr3-octreotate: a new somatostatin analog with improved target tissue uptake. *Nucl Med Biol.* 1999;26:267–273.
25. Siddik ZH. Cisplatin: mode of cytotoxic action and molecular basis of resistance. *Oncogene.* 2003;22:7265–7279.
26. Vekris A, Meynard D, Haaz MC, Bayssas M, Bonnet J, Robert J. Molecular determinants of the cytotoxicity of platinum compounds: the contribution of in silico research. *Cancer Res.* 2004;64:356–362.
27. Oren M. Decision making by p53: life, death and cancer. *Cell Death Differ.* 2003;10:431–442.
28. Ochenduszko SL, Krzemieniecki K. Targeted therapy in advanced colorectal cancer: more data, more questions. *Anticancer Drugs.* 2010;21:737–748.
29. Karapetis CS, Khambata-Ford S, Jonker DJ, et al. K-ras mutations and benefit from cetuximab in advanced colorectal cancer. *N Engl J Med.* 2008;359:1757–1765.
30. Van Cutsem E, Kohne CH, Hitre E, et al. Cetuximab and chemotherapy as initial treatment for metastatic colorectal cancer. *N Engl J Med.* 2009;360: 1408–1417.
31. Van Cutsem E, Oliveira J. Advanced colorectal cancer: ESMO clinical recommendations for diagnosis, treatment and follow-up. *Ann Oncol.* 2009;20 (suppl 4):61–63.
32. Prenen H, Tejpar S, Van Cutsem E. New strategies for treatment of KRAS mutant metastatic colorectal cancer. *Clin Cancer Res.* 2010;16:2921–2926.
33. Bunn PA, Chan D, Stewart J, et al. Effects of neuropeptide analogues on calcium flux and proliferation in lung cancer cell lines. *Cancer Res.* 1994;54:3602–3610.
34. Huang S, Benavente S, Armstrong EA, Li C, Wheeler DL, Harari PM. p53 modulates acquired resistance to EGFR inhibitors and radiation. *Cancer Res.* 2011;71:7071–7079.
35. Huether A, Hopfner M, Baradari V, Schuppan D, Scherubl H. EGFR blockade by cetuximab alone or as combination therapy for growth control of hepatocellular cancer. *Biochem Pharmacol.* 2005;70:1568–1578.
36. Ellis LM, Hicklin DJ. Resistance to targeted therapies: refining anticancer therapy in the era of molecular oncology. *Clin Cancer Res.* 2009;15:7471–7478.
37. Levine AJ, Oren M. The first 30 years of p53: growing ever more complex. *Nat Rev Cancer.* 2009;9:749–758.
38. Valentin J, ed. Radiation dose to patients from radiopharmaceuticals: addendum 3 to ICRP publication 53. ICRP publication 106. *Ann. ICRP.* 38;1–2:1–198.
39. Loke KS, Padhy AK, Ng DC, Goh AS, Divgi C. Dosimetric considerations in radioimmunotherapy and systemic radionuclide therapies: a review. *World J Nucl Med.* 2011;10:122–138.